Bayesian multi-tensor diffusion MRI and tractography

Diwei Zhou[1*], Ian L. Dryden[1], Alexey Koloydenko[1], & Li Bai[2]

[1]School of Mathematical Sciences, Univ. of Nottingham
[2]School of Computer Science and IT, Univ. of Nottingham

1 Introduction

Diffusion tensor imaging (DTI), introduced by Basser *et al.*(1994), is a specific magnetic resonance imaging (MRI) method for brain and many body studies which characterises microscopic structural information of oriented tissue in vivo.

DTI assumes that molecular displacement follows a zero-mean trivariate Gaussian distribution (Alexander, 2005), and its covariance matrix is proportional to the diffusion tensor **D** (see **Table 1**). The eigenstructure of **D** gives the picture of molecular diffusion along different directions (Basser *et al.*, 1994). In particular, the principal eigenvector $\mathbf{v}_1$ corresponding to the largest eigenvalue represents the fibre direction, i.e., DTI can provide a 3-dimensional vector field, and each vector presents the fibre orientation.

The diffusion tensor can be visualised by a diffusion ellipsoid defined by the eigenstructure of **D** (Basser *et al.*, 1994). The diffusion is *isotropic* when water molecular motion is equal and unconstrained in all directions. But, anisotropy may result from the barriers of biological tissue (Le Bihan *et al.*, 2001) where water molecules move along some preferred directions. To quantitatively measure and monitor diffusion anisotropy, scalar quantities derived from **D** have been produced (Le Bihan *et al.*, 2001), such as the mean diffusivity (MD) and Fractional anisotropy (FA) mentioned in **Table 1**.

Term	Meaning
Diffusion tensor (**D**)	$\mathbf{D} = \begin{pmatrix} D_{xx} & D_{xy} & D_{xz} \\ D_{xy} & D_{yy} & D_{yz} \\ D_{xz} & D_{yz} & D_{zz} \end{pmatrix}$ is symmetric (semi)positive-definite. D_{xx}, D_{yy} and D_{zz} represent molecular diffusivities along axes.
Eigenvalues (λ_1, λ_2 and λ_3)	λ_1, λ_2 and λ_3 are positive. Conventionally, let $\lambda_1 \geq \lambda_2 \geq \lambda_3$.
Eigenvectors ($\mathbf{v}_1$, $\mathbf{v}_2$ and $\mathbf{v}_3$)	Unit vectors $\mathbf{v}_1$, $\mathbf{v}_2$ and $\mathbf{v}_3$ are orthogonal. The eigenvectors and eigenvalues coincide with the main diffusion directions and associated diffusivities respectively in the tissue.
Mean diffusivity (MD)	$MD = \frac{\lambda_1+\lambda_2+\lambda_3}{3}$ reflects the isotropic or average degree of diffusion.
Fractional anisotropy (FA)	$FA = \left(\frac{3\times \sum_{k=1}^{3} (\lambda_k - MD)^2}{2\times \sum_{k=1}^{3} \lambda_k^2} \right)^{\frac{1}{2}}$ describes the degree of anisotropy.

Table 1: Glossary of terms

2 Models and Methods of diffusion tensor imaging

2.1 Traditional diffusion tensor models

Under the 3D Gaussian assumption of molecular displacement, the mean μ_i of the resulting diffusion-weighted signal S_i corresponding to the i^{th} diffusion gradient direction $\mathbf{g}_i$ (unit vector) can be obtained from the Fourier transform of the molecular displacement distribution as shown in the diffusion tensor model (Basser *et al.*, 1994).

$$\mu_i = S_0 \exp(-b\mathbf{g}_i^T \mathbf{D}\mathbf{g}_i), i = 1, ..., N, \tag{1}$$

where S_0 is the signal without diffusion gradient applied (i.e.$b = 0$). Roughly, b (b-value) characterises the gradient pulses used in the MRI sequence. For each voxel, the noise of the measured signal is denoted as ε_i. It is assumed that ε_i's are independent and identically distributed (*i.i.d.*) Gaussian variables, $\varepsilon_i \sim \mathbf{N}(0, \sigma^2)$. Thus, the measured signals S_i's are independent Gaussian variables, i.e., $S_i \sim \mathbf{N}(\mu_i, \sigma^2), i = 1, ..., N$.

A generalisation of the diffusion tensor model is the multiple-compartment model (Alexander, 2005), which is proposed to describe the diffusion behaviour in a voxel containing $m \geq 1$ distinct compartments (each compartment has one dominant fibre orientation). Modelling diffusion within the j^{th} compartment by a Gaussian distribution with convariance matrix $\mathbf{D}_j$ and assuming no molecular exchange between compartments, a mixture of the m Gaussians for the overall diffusion process is obtained. The mean of i^{th} diffusion-weighted signal can be modelled as:

$$\mu_i = \sum_{j=1}^{m} a_j S_0 \exp(-b\mathbf{g}_i^T \mathbf{D}_j \mathbf{g}_i), i = 1, ..., N. \tag{2}$$

where the weights $a_j \in (0, 1]$, $\sum a_j = 1, i = 1, ..., N$, of the individual compartments are also known as 'volume fractions'. Hence, by assuming that the noise ε_i's are i.i.d. Gaussian, i.e. $\mathbf{N}(0, \sigma^2)$, the measured signals S_i's are independent $N(\mu_i, \sigma^2), i = 1, ..., N$.

However, we find the parameter set $(a_1, a_1, ..., a_m, \mathbf{D}_1, \mathbf{D}_2, ..., \mathbf{D}_m)$ is not identifiable, i.e., distinct settings of parameters can result in an identical model (Zhou *et al.*, 2008).

2.2 Multi-tensor model

By reparameterising Alexander's (2005) multiple-compartment model, we set up a new multi-tensor model which is identifiable:

$$\mu_i = \begin{cases} \sum_{j=1}^{m} S_0 \exp(-b\mathbf{g}_i^T \mathbf{D}_j^* \mathbf{g}_i) & \text{if } b > 0 \\ S_0 & \text{if } b = 0 \end{cases} \tag{3}$$

where $\mathbf{D}_j^*$ is defined as $\mathbf{D}_j^* = \mathbf{D}_j + q_j \mathbf{I}_{3\times 3}$, and if $b > 0$, $q_j = -\log a_j / b$, $q_j \geq 0$. Obviously, if $b = 0$, then $\mu_i = \sum a_j S_0 = S_0, j = 1.....m$. It can be shown that any $(\mathbf{D}_1^*, \mathbf{D}_2^*, ..., \mathbf{D}_m^*)$ with symmetric (semi) positive-definite $\mathbf{D}_j^*, j = 1...m$, is identifiable as parameters of the multi-tensor model (Zhou *et al.*, 2008). Then, the measured signal S_i can be modelled by adding *i.i.d.* $N(0, \sigma^2)$ noise, ε_i, into the model.

2.3 Bayesian multi-tensor estimation

Least-squares estimation methods have been employed to fit the parameters in traditional diffusion tensor models. Cholesky parametrisation has been explored for guaranteeing positive eigenvalues of **D** (Koay *et al.*, 2006).

For our multi-tensor model, we have developed a Bayesian estimation framework with a new parameterisation of $\mathbf{D}^*$, which takes into account the symmetry and (semi)positive-definiteness of $\mathbf{D}^*$ and incorporates the parameter constraints in the prior beliefs.

The new parameterisation is $\mathbf{D}^* = \mathbf{Q}\mathbf{Q}^T$ where $\mathbf{Q}$ is a general 3x3 matrix. Note that $\mathbf{Q}_j$ and $\mathbf{Q}_j\mathbf{R}_j$ where $\mathbf{R}_j \in O(3)$ result in the same model. Cholesky decomposition is then a special case of our parameterisation. However, we shall actually keep the high dimensional embedding and the matrix $\mathbf{R}_j$ is then a nuisance parameter matrix, which will be controlled through specification of the prior in a Bayesian model.

If there are N acquisitions $\mathbf{S} = (S_1, S_2, ...S_N)$, then Bayesian inference is set up for multi-tensor models with one tensor $(m = 1)$ and two tensors $(m = 2)$.

Model 1:	**Model 2**:
$S_i = S_0 \exp(-b\mathbf{g}_i^T\mathbf{Q}\mathbf{Q}^T\mathbf{g}_i) + \varepsilon_i.$	$S_i = S_0 \exp(-b\mathbf{g}_i^T\mathbf{Q}_1\mathbf{Q}_1\mathbf{g}_i) + S_0 \exp(-b\mathbf{g}_i^T\mathbf{Q}_2\mathbf{Q}_2\mathbf{g}_i) + \varepsilon_i.$
Likelihood:	**Likelihood**:
$L(\mathbf{Q}, \sigma^2) = \prod_{i=1}^{N} f(S_i\|\mathbf{Q}, \sigma^2).$	$L(\mathbf{Q}_1, \mathbf{Q}_2, \sigma^2) = \prod_{i=1}^{N} f(S_i\|\mathbf{Q}_1, \mathbf{Q}_2, \sigma^2).$
Priors:	**Priors**:
$vec(\mathbf{Q}) \sim N_9(vec(\mathbf{I}_{3x3}), \xi^2\mathbf{I}_{9x9}),$	$vec(\mathbf{Q}_1) \sim N_9(vec(\mathbf{I}_{3x3}), \xi_1^2\mathbf{I}_{9x9}),$
$\sigma^2 \sim Inv - Gamma(\alpha, \beta).$	$vec(\mathbf{Q}_2) \sim N_9(vec(\mathbf{I}_{3x3}), \xi_1^2\mathbf{I}_{9x9}),$
	$vec(\mathbf{Q}_1 - \mathbf{Q}_2) \sim N_9(vec(\mathbf{0}_{3x3}), \xi_2^2\mathbf{I}_{9x9}),$
	$\sigma^2 \sim Inv - Gamma(\alpha, \beta).$

Table 2: Bayesian frameworks for multi-tensor models with one tensor ($m = 1$) and two tensors ($m = 2$). $vec(\boldsymbol{Q})$ vectorised $\boldsymbol{Q}$ by stacking the columns of $\boldsymbol{Q}$. $\boldsymbol{I}_{3x3}$ and $\boldsymbol{I}_{9x9}$ are 3x3 and 9x9 identity matrices, respectively.

We will assume large ξ, and so the prior uncertainty about $\mathbf{Q}$ is high. According to Bayes' theorem, we can obtain the posterior distribution $P(\mathbf{Q}, \sigma^2|\mathbf{S})$. By maximising $P(\mathbf{Q}, \sigma^2|\mathbf{S})$, $\mathbf{Q}$ and σ^2 can be estimated. Alternatively, the posterior distribution can be sampled using Markov chain Monte Carlo (MCMC) simulation.

2.4 DTI fibre tractography

Once fibre orientations have been determined from the estimated diffusion tensors for the voxels in a region of interest (ROI), tractography can be used to derive inferences regarding the overall geometry of white matter in the brain. In this paper, we focus on deterministic tractography for the multi-tensor model with one tensor ($m = 1$). Deterministic tractography connects neighboring voxels by propagating the ends of fibre tracts from user-defined seed voxels until termination criteria are met, such as excessive angular deviation of the fibre tracts or subthreshold voxel anisotropy. FA is used as the stopping threshold in the results of this paper.

3 Results

3.1 Simulations

The purpose of this simulation study is to compare three spherical schemes: Philips 15 ($N = 15$), Philips 32 ($N = 32$) and Uniform 32 ($N = 32$) (Sotiropoulos *et al.*, 2008) schemes. The accuracy of DTI measurements depends on diffusion gradient direction scheme applied. A gradient direction scheme is a collection of $\mathbf{g}_i = (g_{ix}, g_{iy}, g_{iz}) \in \mathbf{R}^3$ where N is the number of total directions. For the single tensor model (multi-tensor model with $m = 1$), the defined $\mathbf{D}^*$ is a diagonal matrix with 1,2 and 3 as its eigenvalues and three eigenvectors are along x, y and z axis. We allow $M = 1, 5, 10, 15, 30$ replicates for each of the N directions, and according to the multivariate Gaussian distribution $N(\boldsymbol{\mu}, \sigma^2\mathbf{I}_{N\times N})$, $n = 100$ Monte Carlo simulations were performed for each value of M. The *root mean squared errors* (RMSE) of LLS and Bayesian estimators of single $\mathbf{D}^*$ are shown in **Figure 1**.

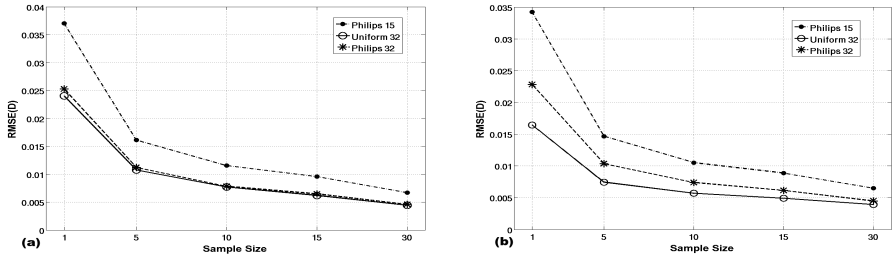

Figure 1: Plots of RMSE of $\mathbf{D}^*$ for three Direction Schemes(M =sample size): (a) RMSE for LLS estimator, (b) RMSE for Bayesian estimator.

3.2 Real data

A set of the MR images with Uniform 32 diffusion gradient direction scheme from a healthy human brain is provided by The Academic Radiology Department of Queen's Medical Centre, University of Nottingham. In this section, the DTI model and multi-tensor model with the Bayesian method are applied for a ROI which is the crossing part of corpus callosum and corona radiata (**Figure 2(a)**). **Figure 2(b)** is the diffusion ellipsoid map from Bayesian single tensor model ($m = 1$) with FA as background. We also carry out the Bayesian estimation for double tensor model ($m = 2$) in **Figure 2(c)**.

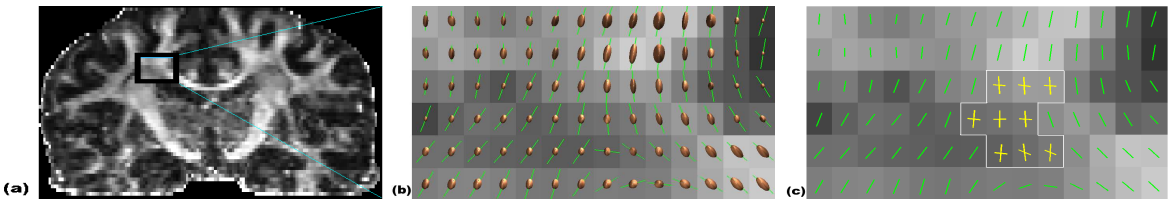

Figure 2: (a) Coronal view of ROI, (b) Ellipsoid map from Bayesian single tensor fitting ($m = 1$) with FA background, (c) Principal eigenvector map from Bayesian double tensor fitting ($m = 2$) with FA background.

3.3 Bayesian tractography

Figure 3 shows the fibre tractography with Bayesian single tensor fitting for the corpus callosum. Such pictures are useful for determining connectivity in the brain.

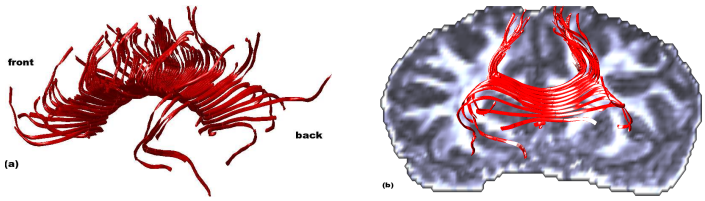

Figure 3: (a) 3D view of fibre tractography for corpus callosum, (b) Coronal view (back-front)of the tractography.

References

Alexander, D.C. (2005). Multiple-fibre Reconstruction Algorithms for Diffusion MRI. *Annals of the New York Academy of Sciences*, **1064**:113-133.

Basser, P.J., Mattiello, J., and Le Bihan, D. (1994). MR Diffusion Tensor Spectroscopy and Imaging. *Biophysical Journal*, **66**: 259-267.

Koay, C.G., Carew, J.D., Alexander, A.L., Basser, P.J., and Meyerand, M.E. (2006). Investigation of Anomalous Estimates of Tensor-Derived Quantities in Diffusion Tensor Imaging. *Magnetic Resonance in Medicine*, **55**: 930-936.

Le Bihan, D., Mangin, J.F., Poupon, C., Clark, C.A., Pappata, S., Molko, N., and Chabriat, H. (2005). Diffusion Tensor Imaging: Concepts and Applications. *Journal of Magnetic Resonance Imaging*, **13**:534-546.

Nucifora, P.G.P., Verma, R., Lee S.K., and Melhem, E.R. (2007). Diffusion-Tensor MR Imaging and Tractography: Exploring Brain Microstructure and Connectivity. *Radiology*, **245**: 367-384.

Sotiropoulos, S.N., Bai, L., Morgan, P.S., Auer, D.P., Constantinescu, C.S. and Tench,C.R. (2008) A Regularized Two-Tensor Model Fit to Low Angular Resolution Diffusion Images Using Basis Directions. *Journal of Magnetic Resonance Imaging* (in press).

Zhou, D., Dryden, I. L., Koloydenko, A., and Bai, L. (2008). A Bayesian method with reparameterisation for diffusion tensor imaging. *Proceedings of SPIE Medical Imaging 2008: Image Processing*, 69142J. Edited by J. M. Reinhardt and J. P. W. Pluim.